Real-time TIRF imaging of exocytosis in 3T3-L1 adipocytes stably expressing mCherry fused to human adiponectin

Man Mohan Shrestha[1], Sebastian Barg[2] and Charlotta S. Olofsson[1]

[1]Department of Physiology/Metabolic Physiology, Institute of Neuroscience and Physiology, Institute of Biochemistry, The Sahlgrenska Academy, University of Gothenburg, Göteborg, Sweden.

[2]Department of Medical Cell Biology, Uppsala University, Uppsala, Sweden.

Running title: *Imaging hormone exocytosis in live adipocytes*

To whom correspondence should be addressed: Dr Man Mohan Shrestha and Associate Professor Charlotta Olofsson, University of Gothenburg, The Sahlgrenska Academy, Dept. Neuroscience and Physiology, Section of Metabolic Physiology, Postal address: Box 432, SE-405 30 Göteborg, Sweden,

E-mail: Man Mohan Shrestha: man.shrestha@gu.se. Charlotta Olofsson: charlotta.olofsson@gu.se

Abstract

Adiponectin is a peptide hormone abundantly released from adipocytes, and its reduced circulating levels have a central role in obesity-related diseases, such as type 2 diabetes, insulin resistance and cardiovascular disease. Adiponectin is secreted by regulated exocytosis of vesicles belonging to a pre-formed vesicle pool, in response to the appropriate stimulatory signal. Traditional molecular biology and imaging techniques lack spatial and temporal resolution to visualize and quantify the exocytosis dynamics of adiponectin-containing vesicles. Here we generate 3T3-L1 adipocytes stably expressing mCherry fused to human adiponectin and we employ total internal reflection fluorescence (TIRF) microscopy in real-time to visualise and quantify exocytosis of the fusion protein. The TIRF recordings show that an intracellular elevation of either cAMP or Ca^{2+}, mediators known to induce adiponectin exocytosis, lead to rapid disappearance of fluorescent vesicles and we interpreted this as exocytosis events. Secretion measurements confirm that the human adiponectin-mCherry fusion protein is secreted to the surrounding solution upon stimulation with agents that elevate intracellular cAMP or Ca^{2+}. We conclude that the fusion protein appear to be directed to vesicles belonging to the endogenous adiponectin vesicle population and that the targeted vesicles are secreted by signals known to stimulate adiponectin exocytosis. Thus, the mCherry-adiponectin-expressing cells are useful for investigations of the adiponectin vesicle exocytosis process in adipocytes, at a level of detail that has not been possible previously.

Introduction

The adipocyte-derived hormone adiponectin has anti-diabetic, anti-atherogenic and anti-inflammatory effects and it acts as an insulin sensitizer. Thus, adiponectin plays crucial roles in metabolic disorders, including insulin resistance, type 2 diabetes and cardiovascular disease [1,2]. Overexpression of adiponectin is associated with protection against both acute and chronic effects of high fat diet-induced lipotoxic effects of lipid accumulation, and enhances the metabolic flexibility of adipose tissue [3].

A number of studies support that adiponectin is secreted via a regulated exocytotic pathway, from a pre-formed vesicle pool. Lim et al. demonstrated the vesicular localisation of adiponectin and that insulin stimulates release of measurable amounts of adiponectin at time-points between 60 and 120 minutes [4]. The insulin-induced secretion was unaffected by pre-incubation with the protein synthesis inhibitor cyclohexamide, indicating that the secretagogue stimulates release of already synthesised adiponectin-containing vesicles. Our own work has defined an alternate pathway for adiponectin exocytosis: By combining electrophysiological and biochemical techniques with mathematical modelling, we have demonstrated that adiponectin exocytosis is triggered by an increase of intracellular cAMP and activation of exchange factor directly activated by cAMP, isoform 1 (Epac1). The cAMP/Epac1- dependent adiponectin vesicle release occurs in the absolute absence of Ca^{2+} (buffering with the Ca^{2+} chelator BAPTA), but is none the less potentiated by an elevation of cytosolic Ca^{2+}. This regulation of adiponectin exocytosis exists in cultured 3T3-L1 adipocytes as well as in primary mouse and human adipocytes. Membrane capacitance recordings (that measure exocytosis as the increase in plasma membrane area that occur upon vesicle fusion) show that the cAMP/Ca^{2+}-triggered adiponectin exocytosis is rapid and initiated within 1-2 min after intracellular addition of stimuli (inclusion of cAMP with or without Ca^{2+} in the patch pipette solution washing into the recorded cell, or extracellular addition of the cAMP-elevating agent forskolin and/or the Ca^{2+} ionophore ionomycin) [5-7]. Later work demonstrated that pre-treatment of adipocytes with the protein synthesis inhibitor cyclohexamide was without effect also on the cAMP-triggered adiponectin release [8]. Collectively, our work proposes that pre-stored adiponectin vesicles undergo rapid exocytosis upon stimulation with cAMP in both the presence and absence of Ca^{2+}, in agreement with the cell model in Fig. 1.

Although capacitance recordings of cell exocytosis is a powerful technique that can provide information about the exocytosis process at high time-resolution, the recordings only give

indirect information regarding the release process (the increase in membrane area resulting from vesicle fusion) and no information about the product secreted or vesicle behavior prior to exocytosis. The exocytosis data can of course be compared to measurements of secreted adiponectin in adipocytes exposed to similar conditions, as we have done previously [6-9]. However, to gain detailed knowledge about the adiponectin exocytosis process and involved regulatory mechanisms, advanced imaging techniques that visualise exocytosis in real time must be used.

Total internal reflection fluorescence (TIRF) microscopy is an elegant optical technique that enables the excitation of fluorophores in a very narrow optical section. TIRF microscopy provides a means to selectively excite fluorophores near the adherent cell surface, while counter-minimizing fluorescent signals from other intracellular regions [10]. The narrow TIRF excitation field allows high-resolution visualisation of processes occurring near or in the plasma membrane, in live cells [11]. Thus, using TIRF microscopy applied to adipocytes expressing a fluorophore localised to adiponectin vesicles, adiponectin containing vesicles that undergo exocytosis can be visually observed at single cell and single vesicle level, at high spatial and temporal resolution.

Here, we describe the generation of 3T3-L1 cells that stably express mCherry fused to the C-terminal end of human adiponectin, to produce a genetically homogenous clonal cell population that sover-express the recombinant protein of interest. We demonstrate that the adiponectin-mCherry expressing cells can be differentiated into mature adipocytes (as judged by lipid-filling) and that TIRF microscopy can be used to visualise and quantify adiponectin exocytosis in real time, at single-vesicle resolution. TIRF recordings show that an intracellular elevation of either cAMP or Ca^{2+} trigger exocytosis of adiponectin-mCherry-labelled vesicles in the stably expressing cells, supported by measurements of secreted adiponectin.

Results

Knock down and rescue of endogenous adiponectin in 3T3-L1 adipocytes

3T3-L1 cells with low passage number were used and it was ascertained that the cells were able to express high levels of endogenous adiponectin when differentiated into adipocytes (Fig. 2A). To avoid that native adiponectin interferes with the expression of human

adiponectin-mCherry, the endogenous adiponectin was knocked down by short hairpin RNA (shRNA). Three different target sequences for shRNA mouse adiponectin knockdown were designed: shAcrp30-A, shAcrp30-B and shAcrp30-C (Table 1). The targets were inserted into a lentiviral plasmid and 3T3-L1 fibroblasts were transduced with the viral particles. The transduced cells were thereafter differentiated into mature adipocytes. For two out of three knockdowns, shAcrp30-A and shAcrp30-C, transduced cells could be cultured into mature adipocytes whereas cells transduced with shAcrp30-B did not survive. The successful knockdown was confirmed by protein and gene expression, where adiponectin gene knockdown was compared with scrambled shRNA targeting GFP (Fig. 2B-D).

Cells that displayed the most efficient knockdown (shAcrp30-A), were rescued with hAcrp30-mCherry alone (plasmid map in Suppl. Fig. 1A) or with a FLAG tag either at the N- or C-terminal in the fibroblast stage. The FLAG was added to allow future protein purification by affinity chromatography as well as localisation of the fusion protein in live cells. The rescued cells were seeded and differentiated into mature adipocytes, and the over-expression of hAcrp30 was verified by Western blotting using antibodies against adiponectin or FLAG. The hAcrp30-mCherry tagged with FLAG at the C-terminal was found to be highly over-expressed compared to the other two variants under both reduced (Fig. 3A) and non-reduced (Fig. 3B) conditions. The over-expression of adiponectin-mCherry was visualized by inverted fluorescence microscope (Fig. 3C) and TIRF microscopy. TIRF imaging demonstrated a punctate pattern of fluorescence, as typical for vesicular compartments (Fig. 3D).

An elevation of intracellular cAMP or Ca^{2+} triggers exocytosis of mCherry-labelled adiponectin vesicles

By combining electrophysiological recordings with secretion measurements, we have previously shown that adiponectin vesicle exocytosis is stimulated by an elevation of cAMP and Ca^{2+} [6,7]. We have also demonstrated that a combination of the adenylyl cyclase activator forskolin and the phosphodiesterase inhibitor 3-isobutyl-1-methylxanthine (FSK/IBMX) increases 3T3-L1 adipocyte cAMP levels >6-fold [7] and that the Ca^{2+} ionophore ionomycin elevates the intracellular Ca^{2+} level ($[Ca^{2+}]_i$; [6]). Thus, we investigated adiponectin vesicle exocytosis in differentiated 3T3-L1 adipocytes stably expressing adiponectin-mCherry exposed to FSK/IBMX or ionomycin. As shown in Fig. 4A, addition of FSK/IBMX triggered exocytosis of mCherry-labelled vesicles, visualised as the rapid disappearance of fluorescent vesicles (bottom images in Fig. 4A and Suppl. video 1). A rapid loss of fluorescence puncta

upon stimulation was observed, which we interpreted as exocytosis events (top row Fig. 4C and Fig. 4D). Approx. 40% of the vesicles did not fuse with the plasma membrane after addition of the stimulatory agents, but instead remained stable throughout the recording (middle row Fig. 4C and Fig. 4E). This is expected since all adiponectin vesicles that reside close to the plasma membrane, within the TIRF zone, are unlikely to be primed for exocytosis [12]. In control experiments using cells that were exposed to the control solution during the entire experiment (Fig. 4B and Suppl. video 2), the labelled adiponectin vesicles remained stable throughout the TIRF recording (bottom row Fig. 4C). Calculation of the fraction of released vesicles in FSK/IBMX and control experiments demonstrated that a larger number of vesicles were exocytosed at different time-points upon exposure to the cAMP-elevating agents (Fig. 4F). At the end of 15 minutes recordings, significantly fewer adiponectin-mCherry labelled vesicles remained in adipocytes exposed to FSK/IBMX, compared to control cells (Fig. 4G).

Application of the Ca^{2+} ionophore ionomycin (potently elevates intracellular Ca^{2+} levels) likewise triggered the exocytosis of adiponectin-containing vesicles (Fig. 5A, and Suppl. video 3). Similar to the experiments with FSK/IBMX, a rapid loss of fluorescence puncta was observed upon stimulation, indicating vesicle exocytosis (top row Fig. 5C and Fig. 5D) and a fraction of adiponectin-containing vesicles remained stable throughout the recording (middle row Fig. 5C and Fig. 5E). Control experiments (no addition of ionomycin) again showed that the adiponectin-mCherry vesicles remained stable under control conditions (Fig. 5B, bottom row Fig. 5C and Suppl. video 4). The fraction of released vesicles were significantly larger in the ionomycin-exposed adipocytes compared to control experiments at all investigated time-points (Fig. 5F). As in experiments with FSK/IBMX, significantly fewer adiponectin-mCherry labelled vesicles remained in ionomycin-exposed adipocytes compared to control cells, at the end of 15 minute recordings (Fig. 5G). The number of adiponectin containing vesicles released per area (vesicles/μm^2) were similar in 3T3-L1 adipocytes exposed to FSK/IBMX or ionomycin (Suppl. Fig. 1B).

Measurements of adiponectin secretion in 3T3-L1 adipocytes stably expressing mCherry-adiponectin

To verify the adiponectin secretion capacity of the stably transduced 3T3-L1 cells, the matured adipocytes were incubated in the presence of FSK/IBMX or ionomycin and secreted product was measured by ELISA. In agreement with previous results (Komai 2014; El Hachmane 2015)

the secretagogues stimulated the release of mouse adiponectin in native 3T3-L1 adipocytes (Fig. 6A). The 3T3-L1 adipocytes stably expressing adiponectin-mCherry (bright field example of cell in Fig. 6B) likewise secreted adiponectin in response to both FSK/IBMX and ionomycin and both total (Fig. 6C) and the high-molecular weight (HMW) form (Fig. 6D) of human adiponectin were released over basal (unstimulated control cells). The data confirm that the stably expressing adipocytes secrete the adiponectin-mCherry fusion protein in response to stimulation with FSK/IBMX or ionomycin, at levels similar to that observed for mouse adiponectin release in native cells.

Discussion

Pre-stored neurotransmitter- or hormone-containing secretory vesicles typically release their content to the extracellular space, when receiving the correct triggering signal. Classically, an elevation of intracellular Ca^{2+}, released from intracellular stores or transported in via Ca^{2+}-permeable channels in the plasma membrane, stimulates vesicle exocytosis; other intracellular mediators such as cAMP and ATP have important roles for the vesicle secretion [12]. Peptide hormone exocytosis has been investigated in detail in a large number of endocrine cell types, including insulin secreting beta-cells [13] and catecholamine-releasing chromaffin cells [14]. However, the control of hormone release in white adipocytes is a research field that has received limited attention. Adiponectin, one of the chief hormones secreted from white adipocytes, has in several studies been reported to have favourable metabolic effects and to protect from development of metabolic diseases, such as type 2 diabetes [1,2]. Although the general control of adiponectin secretion over shorter and longer time-periods has been addressed in a small number of studies [4,15-17], adiponectin vesicle exocytosis – the molecular and cellular process in which adiponectin-containing vesicles fuse with the adipocyte plasma membrane to release their cargo to the extracellular space - is a largely unexplored field. Here we demonstrate the successful generation of 3T3-L1 cells stably expressing human adiponectin fused with the fluorescent protein mCherry. Below we discuss potential benefits and concerns associated with the generation of the adiponectin-mCherry-expressing cells, as well as advantages and limitations associated with their future usage for detailed studies of the adiponectin exocytosis process.

Choice of cells and fluorescent protein

In this study, 3T3-L1 cells were used to generate the adiponectin-mCherry expressing adipocytes. A number of studies have demonstrated that *in vitro* differentiated 3T3-L1 adipocytes are a relevant cell model for investigations of the adiponectin secretion process [5-7,9,18]. In fact, all mechanisms and mediators determined to regulate adiponectin exocytosis in 3T3-L1 adipocytes have been confirmed in primary mouse and human adipocytes ([7-9] and Musovic & Olofsson, unpublished data). The 3T3-L1 adipocytes are easy to culture and differentiate, and their functionality with regard to adipocyte metabolic processes, such as lipolysis [19] and glucose uptake [20], is well determined. Nonetheless, the 3T3-L1 adipocytes are clonal cells and we acknowledge that results must continuously be confirmed in experiments with primary, preferably human, adipocytes. A disadvantage with the 3T3-L1 adipocytes is that their ability to differentiate into mature adipocytes ceases with increased cell passage. Although we have stored multiple vials of low passage cells, we will eventually need to produce new stably expressing 3T3-L1 cells in the future. We are however not aware of any adipocyte cell line that does not have this problem; thus, we regarded the 3T3-L1 adipocytes to be a good choice.

A large number of fluorescent proteins are available for protein tagging, to allow real-time studies of their specific function. The continuous development of fluorescent proteins with enhanced or altered qualities have generated a supply that covers the full visible spectrum, with diverse advantages and disadvantages. Introduced nearly a decade ago, mCherry remains a frequently used fluorescent protein for cellular studies. The advantages of mCherry is that it is bright and that it matures rapidly, thus making it possible to carry out experiments soon after initiation of expression. mCherry is also highly photostable and resistant to photobleaching [21]. Since we want to perform experiments at high-time resolution and over an extended time-period (up to 30 min) the listed qualities are important. We therefore labelled adiponectin with mCherry, expressed under the CMV promoter that has high housekeeping expression. Human adiponectin was chosen to enable us to biochemically distinguish between endogenous mouse adiponectin and the overexpressed fusion protein.

However, there are some disadvantages related to using mCherry for studies of adiponectin exocytosis: Red fluorescent proteins, including mCherry, display limited pH sensitivity compared to e.g. enhanced green fluorescent protein (EGFP) or pHluorin. Upon vesicle fusion with the plasma membrane the pH of the vesicle lumen (which is acidic) increases; pH-

sensitive fluorescent proteins will consequently increase in brightness already upon formation of the vesicle-plasma membrane fusion pore, thus confirming that vesicle fusion occurs. For this reason, we initially evaluated the use of EGFP for studies of adiponectin exocytosis. However, we found that both the more rapid photobleaching of EGFP compared to mCherry, as well as lipid autofluorescence interfering with the green signal created problems. Due to that pHluorin is non-fluorescent at low pH, we were reluctant to test this optical indicator in our first studies. We nonetheless acknowledge that the advantage of using a pH-sensitive fluorescent tag for studies of vesicle fusion and cargo release prompts us to evaluate their use for future investigations of the adiponectin secretion process. We also recognise that tagging adiponectin itself might interfere with both protein mulitmerisation and the secretion process. However, our secretion data demonstrate that the stably expressing adipocytes release abundant amounts of HMW adiponectin, verifying that multimerisation of the chimeric protein is possible. Nonetheless, it would be valuable to assess if labelling of another exocytosis vesicle marker, such as Neuropeptide Y (NPY) that is a reliable marker for insulin granule exocytosis [21], is useful for TIRF investigations of adiponectin vesicle release.

The adiponectin-mCherry protein is targeted to vesicles belonging to the endogenous adiponectin vesicle population

Upon interference with a protein by addition of a fluorescent tag there are of course concerns that this can disturb the correct targeting of the product. The TIRF data propose that the chimeric protein is present in vesicular compartments, indicated by the punctate appearance of the fluorescence signal. The real-time recordings moreover suggest that the overexpressing adipocytes are functional, and that adiponectin-mCherry is targeted to the correct vesicle population, as shown by that the labelled vesicles fuse with the plasma membrane in response to signals known to stimulate adiponectin exocytosis. In further support of this, the live imaging data are supported by measurements of secreted human adiponectin, demonstrating that the fusion protein is secreted in response to an elevation of cAMP or Ca^{2+}, just like endogenously expressed adiponectin. We have shown that secretion of the hormones leptin, apelin and adipsin is unaffected by cAMP in 3T3-L1 adipoytes (5) and that resistin is co-secreted with adiponectin (contained within the same vesicles (37)). Collectively, our data support that the rapid loss of fluorescence puncta in response to an intracellular elevation of cAMP or Ca^{2+} reflects exocytosis of vesicles belonging to the endogenous adiponectin vesicle population. Fig. 4 demonstrates our ability to visualise, analyse and quantify adiponectin exocytosis events at the single vesicle level.

Both cAMP and Ca^{2+} trigger exocytosis of adiponectin-mCherry labelled vesicles

Using a combination of patch-clamp recordings of 3T3-L1 adipocyte exocytosis (increases in membrane capacitance) and biochemical measurements of secreted adiponectin, we have previously demonstrated that adiponectin exocytosis occurs when intracellular cAMP increases and activates Epac1. The cAMP-stimulated adiponectin exocytosis is maintained under Ca^{2+}-free conditions (inclusion of the Ca^{2+} chelator BAPTA in the pipette solution rinsing in to the patched cell or pre-treatment of adipocytes with membrane permeable BAPTA-AM) but an elevation of intracellular Ca^{2+} none the less potently augments cAMP-triggered adiponectin exocytosis. Moreover, Ca^{2+} and ATP are essential for replenishment of the pool of releasable adiponectin vesicles, and thus for maintenance of adiponectin secretion over extended time-periods [5-7,22] (Fig. 1).

The real-time TIRF imaging data in Figs. 4 and 5 confirm the importance of cAMP and Ca^{2+} for stimulation of adiponectin vesicle release. However, the results in Fig. 5 where the Ca^{2+} elevation induced by ionomycin can appear to contradict the previous results demonstrating that Ca^{2+} alone is unable to induce exocytosis in cAMP-depleted 3T3-L1 adipocytes. Importantly, there are some essential difference between our previous patch-clamp data and current TIRF recordings. The electrophysiological experiments are rather invasive as the interior of the adipocytes is controlled by the pipette solution – thus cells can be essentially depleted of excluded mediators, such as cAMP. In contrast, the adipocytes used for TIRF imaging are metabolically intact and have a continuous endogenous production of cAMP, maintaining basal levels of the cyclic nucleotide. We hypothesise that the preserved endogenous levels of cAMP act together with the elevated Ca^{2+} to stimulate adiponectin exocytosis. The finding that ionomycin on its own stimulates adiponectin secretion in metabolically intact adipocytes is in agreement with data on secretion of resistin, another adipocyte hormone [23]; we recently showed that resistin is co-secreted with adiponectin in mouse adipocytes (thus contained within the same vesicles) and that ionomycin induced the release of resistin in the absence of a cAMP elevating agent [24]. An alternative explanation to the effect of ionomycin alone is that the increase in intracellular Ca^{2+} activates Ca^{2+}-dependent adenylyl cyclases leading to production of cAMP. In Musovic et. al. 2021 we were unable to demonstrate a significant increase of cAMP levels in 3T3-L1 adipocytes exposed to ionomycin (Fig. 1C of [24]). However, cAMP was measured in cell lysates and this is a rather crude method that does not provide information of local changes of cAMP, in specific near-membrane

regions. It is thus possible that ionomycin stimulates local elevations of cAMP, at sites of adiponectin vesicle exocytosis. It is well known that cAMP is compartmentalised in adipocytes and that this regulates several intracellular processes [25]. In cardiac myocytes, a role of caveolae in the spatial control of cAMP has been demonstrated and proposed to be relevant for βAR signalling [26]. We have previously shown that caveolae are essential for the organisation of signalling pathways involved in the regulation of HMW adiponectin exocytosis [27].

TIRF imaging visualises a small cytoplasmic region adjacent to the plasma membrane

Vesicles that contain peptide/protein hormones typically undergo a series of maturation steps including physical movement, docking (stable attachment to the plasma membrane) and priming (chemical modifications that make docked vesicles release competent) before they can discharge their cargo upon fusion with the plasma membrane [12]. Looking at the data in Figs. 4 and 5 as well as supplementary videos 1 and 2, it can be seen that both cAMP and Ca^{2+} appear to trigger exocytosis of adiponectin vesicles that are already docked at the adipocyte plasma membrane; no new vesicles (newcomers) entering the TIRF zone can be seen. This observation appears to stand in conflict with our previous electrophysiological data demonstrating that an elevation of Ca^{2+} maintains adiponectin secretion over time and our conclusion that Ca^{2+} induces vesicle replenishment. In this context, it is essential to keep in mind that we image only only a part of/near the adipocyte plasma membrane, the ventral side of the cell attached to the culture dish, whereas the capacitance recording reflect exocytosis that occur over the entire cell membrane. Consequently, vesicles that move to and undergo exocytosis at the apical side of the plasma membrane, outside of the TIRF imaging zone, are not included in the analysis.

The fact that we visualise only a fraction of the plasma membrane and its near cytoplasmic region can also explain that a similar amount of adiponectin is released upon stimulation with FSK/IMBX or ionomycin (Figs. 6A-D), although the rate of adiponectin vesicle fusion is clearly higher in response to cAMP compared to Ca^{2+}. Our data suggest that ionomycin might induce more potent secretion of adiponectin at sites that differ from those involved in the cAMP-triggered exocytosis, perhaps in membrane regions not attached to the cell culture dish.

What can we learn about the control of adiponectin secretion by real-time TIRF imaging of adiponectin exocytosis?

Using a combination of electrophysiological and biochemical methods as well as mathematical modelling, we have begun to detail the white adipocyte adiponectin exocytosis process [5-9,18,22,28]. However, those methods have temporal and spatial limitations and detailed knowledge of adiponectin vesicle dynamics and release can only be gained by imaging in live cells. The finding that 3T3-L1 is a good adipocyte model open opportunities to use our stably expressing cells to gain a comprehensive understanding of mechanisms and mediators that control adiponectin vesicle exocytosis, at the cellular and molecular level. Recordings of TIRFM movies can be acquired at high time resolution (10-20 FPS), thus allowing real time direct visualisation of the adiponectin vesicle exocytosis process; the control and rate of docking and exocytosis can be determined. How are adiponectin vesicles recruited to the exocytosis site? Are the vesicles present before, during and after exocytosis? Do vesicles interact with each other during the exocytosis process? Those are questions that we will be able to answer. Are β_3AR or Epac1recruited/interact with each other or with adiponectin vesicles at the exocytosis site before or during adiponectin vesicle fusion? This can be determined in 3T3-L1 adipocytes that co-express fluorescently labelled β_3AR or Epac1. Studies in pancreatic β-cells have shown that Epac2 controls the expansion of the fusion pore and thereby insulin release during insulin granule exocytosis [29].

Extending the investigations to a more pathophysiological setting, similar studies can be done in primary human and mouse adipocytes. *In vivo* adipose tissue-targeted adeno-associated virus (AAV) can be done in lean and obese/diabetic mice, for studies of adiponectin vesicle dynamics and exocytosis in freshly isolated primary adipocytes that overexpress fluorescently labelled adiponectin, or another vesicle marker. AAV-based vectors have high *in vivo* transduction efficiency, with long-lasting protein overexpression [30]. Fat pad-specific microinjections will allow investigations of inguinal (subcutaneous) or gonadal (visceral) adipocytes and results in "lean" or "obese adipocytes" can be compared to whole-body metabolic health. The experiments can answer questions such as: Are fewer adiponectin vesicle recruited/docked in obese adipocytes or is vesicle fusion halted before the cargo is released? Also, human primary adipocytes can be transiently transfected to express an adiponectin fluorescent vesicle marker. This *ex vivo* approach is feasible in human fat cells, since they stay viable and functional in culture over 24-48 hours.

In summary, TIRF imaging of cultured or primary live adipocytes with fluorescently labelled adiponectin vesicles will enable us, and others, to define currently unknown regulatory steps of adiponectin exocytosis, at the single vesicle level. Future experiments will thus provide answers to a number of questions that can not be solved using electrophysiological or biochemical techniques.

Methods

Safety and Handling of Recombinant Lentiviruses

All the lentiviruses were generated using a third generation packaging system as per Biosafety Level 2 and institutional guidelines of the University of Gothenburg. Disposable plastic pipettes were used and liquid waste was decontaminated with 10 % bleach. Laboratory materials in contact with viral particles were treated as biohazardous waste and autoclaved.

Cell culture

HEK293T (ATCC) cells were cultured in high glucose DMEM (Invitrogen, GIBCO) supplemented with 10 % fetal bovine serum (FBS) and 1 % penicillin-streptomycin at 37 ^{0}C and 5 % CO_2. Cultured clonal 3T3-L1 fibroblasts (Zenbio) were seeded and differentiated into mature adipocytes and used for experiments at day 8 or 9 according to previous establish protocol [7]. In brief, 3T3-L1 fibroblasts were cultured in high glucose DMEM (Invitrogen, GIBCO) supplemented with 10 % new born calf serum at 37 ^{0}C and 5 % CO_2. Two days after confluence, cells were washed twice with warm PBS and a differentiation medium containing 10 % FBS, 1 % penicillin-streptomycin, 0.85 μM insulin, 0.5 mM 3-isobutyl-1-methylxanhine and 1 μM dexamethasone was added for 2 days. The differentiation medium was there after replaced with medium containing 10 % FBS and insulin for another 2 days. Cells were then maintained in DMEM with 10 % FBS. Adipocytes were used for experiments on day 8 or 9 post differentiation. Only 3T3-L1 adipocytes that appeared mature, as judged visually by accumulated lipid, were studied.

Generation of lentiviral constructs

Three candidate hairpin sequences for mouse adiponectin (NM_009605.5) each containing 21 sense bases that are identical to the target gene, a loop containing an XhoI restriction site and

21 antisense bases that are complementary to the sense bases followed by a poly T termination sequence, were designed using an small interfering RNA (siRNA) selection tool hosted by the Whitehead Institute for Biomedical Research (http://sirna.wi.mit.edu/) [31]. Starting at 25nt downstream of the start codon (ATG), we searched for 21nt sequences that matched the pattern AA(N19). It was ascertained that the G-C content was >35 %. To minimize degradation of off-target mRNAs, the NCBI's BLAST program was used. Since some sequences are likely more effective than others, multiple target sequences were selected for the *Acrp30* gene (Table 1).

The annealed oligos were inserted into an empty backbone third generation transfer plasmid (pLKO.1-TRC cloning vector; Plasmid #10878; addgene) using AgeI (5' cloning site) and EcoRI (3' cloning site) restriction digestion sites. Similarly, a candidate hairpin sequence for green fluorescent protein (GFP) was used for a control/scramble (pLKO.1 GFP; Plasmid #30323; addgene). mCherry fused to human adiponectin (hAcrp30-mCherry) was cloned into a pLenti vector using NheI and HpaI restriction digestion sites to generate lentiviral constructs (Supplementary Fig. 1A). The sequences of the knockdown and lentiviral constructs were verified using restriction digestion and Sanger's Sequencing from Eurofins Genomics.

Lentivirus Packaging and Infection

Lentiviruses were produced by co-transfection of HEK293T cells with lentiviral expression and packaging plasmids using the calcium phosphate transfection method [32,33]. Viral supernatant was collected after 48 hours of transfection, centrifuged at 1,000 x g for 5 minutes and filtered through 0.45 µm filter. The viruses were further concentrated by ultracentrifugation using Ti45 rotor in Beckman Coulter Optima-L-100 XP at 116,000 x g for 2 hours at 4 °C. For gene silencing, 3T3-L1 fibroblasts were transduced with titrated viruses in presence of 8 µg/mL of polybrene (Hexadimethrine bromide, Cat. No: 107689-10G, SIGMA-ALDRICH) and subjected to antibiotic selection using 4 µg/mL puromycin after 48 hours. The successful stable expression was verified by fluorescence microscopy for fusion proteins whereas knockdown efficiency was assessed by Western blotting and RT-qPCR at protein and mRNA level respectively. For generation of a stably expressing mCherry fused adiponectin cell line, 3T3-L1 fibroblasts were infected with optimum amount of viral particles in the presence of polybrene. The growth medium was changed 24 hours after infection.

Adiponectin secretion

3T3-L1 cells stably expressing mCherry-adiponectin were seeded and differentiated into mature adipocytes on 35 mm glass bottom dish (D35-20-1.5-N, Cellvis). The mature adipocytes were incubated with an extracellular (EC) solution containing 140 mM NaCL, 3.6 mM KCL, 0.5 mM $MgSO_4$, 0.5 mM NaH_2PO_4, 2.0 mM $NaHCO_3$ and 5.0 mM Hepes (pH 7.4) supplemented with 2.6 mM $CaCl_2$ and 5.0 mM glucose for 30 minutes at 32 °C. Test substances were added for 30 min at 32 °C under gentle shaking. At termination of the incubation, the medium containing secreted product was collected, and the adipocytes were lysed using PBS containing 2 % SDS and protease inhibitor (1 tablet per 10 mL; cOmplete Mini, Roche Diagnotics. Secretion samples were centrifuged for 5 minutes at 2000 rpm and 4 ^{0}C, and the supernatant was stored at -80 °C. Secreted HMW and total adiponectin (measured with HMW and Total Adiponectin ELISA (human) kit, 47-ADPMS-E01, Alpco) were expressed in relation to total protein content. Cell lysates were centrifuged at 14000 rpm for 10 minutes at 4 ^{0}C and total protein contents were measured by Bradford protein assay.

Real-Time Quantitative PCR

RNA was extracted and purified using QIAzol (Qiagen) and ReliaPrep RNA Cell MiniPrep System (Promega). 1 µg of RNA was used for reverse transcription. cDNA synthesis was performed according to the protocol as described in Invitrogen^{TM} SuperScript^{TM} II Reverse Transcriptase kit (Thermo Fisher Scientific #18064022) in presence of 40 units of RNaseOUT^{TM} Recombinant Ribonuclease Inhibitor (Thermo Fisher Scientific #10777-019) and 200 units of Reverse Transcriptase per 20 µL of reaction mixture. The real-time quantitative PCR (qPCR) assays were performed using Fast SYBR Master Mix (4385612, Applied Biosystems). The relative expression of mRNA abundance was calculated using $2^{-\Delta\Delta Ct}$ and was normalized to β-actin. Data are represented as mean ± SEM, ****$p<0.0001$ (n=3).

Western blotting

3T3-L1 adipocytes were lysed with TNET buffer (50 mM Tris-HCl, pH 7.5, 150 mM NaCl, 10 mM NaF, 1 mM EDTA and 1% Triton X-100) containing 2 mM Na_3VO_4 (Sodium Orthovanadate) and 1 mM pmsf (phenylmethylsulfonyl fluoride) and 1x protease inhibitor cocktail tablet (Roche). Whole cell lysates were centrifuged at 12,000 rpm at 4 ^{0}C for 10 minutes. The protein concentration was determined using Bradford protein assay. Proteins from whole cell lysate (20 µg) were separated by 8 % sodium dodecyl sulfate polyacrylamide

gel electrophoresis (SDS/PAGE) and then transferred onto polyvinylidene difluoride (PVDF) membranes (Millipore) at 120 V for 2 hours using transfer buffer (25 mM Tris-base, pH 8.3, 190 mM glycine, 20 % methanol and 0.1 % SDS). After blocking in blocking buffer (2 % BSA in PBS containing 0.2 % Tween-20 and 0.01 % sodium azide) for 1 hour at room temperature, the membrane was incubated overnight at 4 ^{0}C with primary antibody against adiponectin (ab3455, Abcam) and tubulin (T9026, Sigma) as loading control at 1:1000 dilution. The primary antibodies were probed using HRP-conjugated secondary antibodies at 1:5000 dilution and detection was performed with enhanced chemiluminescence.

Live Cell imaging by TIRF microscopy and vesicle exocytosis analysis

3T3-L1 adipocytes expressing hAcrp30-mCherry were pre-treated with EC for 30 minutes at 32 °C and kept in the same solution supplemented with 2.6 mM $CaCl_2$ and 5.0 mM glucose during imaging. Image acquisition was performed by TIRF Observer Z1 microscope with alpha Plan-Apochromat 100×/1.46 Oil objective (both Carl Zeiss) and an EMCCD camera (Evolve 512 delta, Photometrics). Images were acquired using Zeiss Zen 2.6 (blue edition). Excitation laser of wavelength 561 nm with exposure time 25–100 ms was used for mCherry. Forskolin together with the phosphodiesterase inhibitor 3-isobutyl-1-methylxanthine (FSK/IBMX) or ionomycin alone were added 1–2.5 minutes after acquisition start and the time point was noted. TIRF images were acquired over 15 minutes at 2 Hz through 1801 total readings. Circles of region of interest (ROI) around the vesicles were used to measure the fluorescence intensities of images over time. All the readings were normalized to the intensity measured at time point zero, after removal of the background fluorescence. Values were plotted against time, so as to indicate the time course of adiponectin containing vesicle exocytosis.

Analysis

Images were analysed by using Zeiss Zen 2.6 (blue edition). All data are presented as mean values ± SEM for designated number of experiments. Significance of difference was tested by Student's t-test and ANOVA. All statistical analysis were performed using Prism 9.0 (GraphPad, San Diego, CA).

References

1 Straub, L. G. & Scherer, P. E. Metabolic Messengers: Adiponectin. *Nat Metab* **1**, 334-339, doi:10.1038/s42255-019-0041-z (2019).

2 Iwabu, M., Okada-Iwabu, M., Yamauchi, T. & Kadowaki, T. Adiponectin/AdipoR Research and Its Implications for Lifestyle-Related Diseases. *Front Cardiovasc Med* **6**, 116, doi:10.3389/fcvm.2019.00116 (2019).

3 Combs, T. P. *et al.* A transgenic mouse with a deletion in the collagenous domain of adiponectin displays elevated circulating adiponectin and improved insulin sensitivity. *Endocrinology* **145**, 367-383, doi:10.1210/en.2003-1068 (2004).

4 Lim, C. Y., Hong, W. & Han, W. Adiponectin is released via a unique regulated exocytosis pathway from a pre-formed vesicle pool on insulin stimulation. *Biochem J* **471**, 381-389, doi:doi.org/10.1042/BJ20150301 (2015).

5 Brannmark, C. *et al.* Mathematical modeling of white adipocyte exocytosis predicts adiponectin secretion and quantifies the rates of vesicle exo- and endocytosis. *J Biol Chem* **292**, 20032-20043, doi:10.1074/jbc.M117.801225 (2017).

6 El Hachmane, M. F., Komai, A. M. & Olofsson, C. S. Cooling Reduces cAMP-Stimulated Exocytosis and Adiponectin Secretion at a Ca2+-Dependent Step in 3T3-L1 Adipocytes. *PLoS One* **10**, e0119530, doi:10.1371/journal.pone.0119530 (2015).

7 Komai, A. M., Brannmark, C., Musovic, S. & Olofsson, C. S. PKA-independent cAMP stimulation of white adipocyte exocytosis and adipokine secretion: modulations by Ca2+ and ATP. *J Physiol* **592**, 5169-5186, doi:10.1113/jphysiol.2014.280388 (2014).

8 Komai, A. M. *et al.* White Adipocyte Adiponectin Exocytosis Is Stimulated via beta3-Adrenergic Signaling and Activation of Epac1: Catecholamine Resistance in Obesity and Type 2 Diabetes. *Diabetes* **65**, 3301-3313, doi:10.2337/db15-1597 (2016).

9 Musovic, S. *et al.* Noradrenaline and ATP regulate adiponectin exocytosis in white adipocytes: Disturbed adrenergic and purinergic signalling in obese and insulin-resistant mice. *Mol Cell Endocrinol* **549**, 111619, doi:10.1016/j.mce.2022.111619 (2022).

10 Mattheyses, A. L., Simon, S. M. & Rappoport, J. Z. Imaging with total internal reflection fluorescence microscopy for the cell biologist. *J Cell Sci* **123**, 3621-3628, doi:10.1242/jcs.056218 (2010).

11 Burchfield, J. G., Lopez, J. A., Mele, K., Vallotton, P. & Hughes, W. E. Exocytotic vesicle behaviour assessed by total internal reflection fluorescence microscopy. *Traffic* **11**, 429-439, doi:10.1111/j.1600-0854.2010.01039.x (2010).

12 Burgoyne, R. D. & Morgan, A. Secretory granule exocytosis. *Physiol Rev* **83**, 581-632, doi:10.1152/physrev.00031.2002 (2003).

13 MacDonald, P. E. & Rorsman, P. The ins and outs of secretion from pancreatic beta-cells: control of single-vesicle exo- and endocytosis. *Physiology (Bethesda)* **22**, 113-121, doi:10.1152/physiol.00047.2006 (2007).

14 Garcia, A. G., Garcia-De-Diego, A. M., Gandia, L., Borges, R. & Garcia-Sancho, J. Calcium signaling and exocytosis in adrenal chromaffin cells. *Physiol Rev* **86**, 1093-1131, doi:10.1152/physrev.00039.2005 (2006).

15 Cong, L. *et al.* Regulation of adiponectin and leptin secretion and expression by insulin through a PI3K-PDE3B dependent mechanism in rat primary adipocytes. *Biochem J* **403**, 519-525, doi:10.1042/BJ20061478 (2007).

16 Bogan, J. S. & Lodish, H. F. Two compartments for insulin-stimulated exocytosis in 3T3-L1 adipocytes defined by endogenous ACRP30 and GLUT4. *J Cell Biol* **146**, 609-620, doi:10.1083/jcb.146.3.609 (1999).

17 Xie, L., O'Reilly, C. P., Chapes, S. K. & Mora, S. Adiponectin and leptin are secreted through distinct trafficking pathways in adipocytes. *Biochim Biophys Acta* **1782**, 99-108, doi:10.1016/j.bbadis.2007.12.003 (2008).

18 Lovfors, W. *et al.* A systems biology analysis of adrenergically stimulated adiponectin exocytosis in white adipocytes. *J Biol Chem* **297**, 101221, doi:10.1016/j.jbc.2021.101221 (2021).
19 Zhang, X., Heckmann, B. L. & Liu, J. Studying lipolysis in adipocytes by combining siRNA knockdown and adenovirus-mediated overexpression approaches. *Methods Cell Biol* **116**, 83-105, doi:10.1016/B978-0-12-408051-5.00006-1 (2013).
20 Nugent, C. *et al.* Potentiation of glucose uptake in 3T3-L1 adipocytes by PPAR gamma agonists is maintained in cells expressing a PPAR gamma dominant-negative mutant: evidence for selectivity in the downstream responses to PPAR gamma activation. *Mol Endocrinol* **15**, 1729-1738, doi:10.1210/mend.15.10.0715 (2001).
21 Gandasi, N. R. *et al.* Survey of Red Fluorescence Proteins as Markers for Secretory Granule Exocytosis. *PLoS One* **10**, e0127801, doi:10.1371/journal.pone.0127801 (2015).
22 Komai, A. M., Shrestha, M. M., Musovic, S. & Olofsson, C. S. An Approach to Monitor Exocytosis in White Adipocytes. *Methods in molecular biology* **2233**, 203-222, doi:10.1007/978-1-0716-1044-2_14 (2021).
23 Park, H. K. & Ahima, R. S. Resistin in rodents and humans. *Diabetes Metab J* **37**, 404-414, doi:10.4093/dmj.2013.37.6.404 (2013).
24 Musovic, S., Shrestha, M. M., Komai, A. M. & Olofsson, C. S. Resistin is co-secreted with adiponectin in white mouse adipocytes. *Biochem Biophys Res Commun* **534**, 707-713, doi:10.1016/j.bbrc.2020.11.013 (2021).
25 Rogne, M. & Tasken, K. Compartmentalization of cAMP signaling in adipogenesis, lipogenesis, and lipolysis. *Hormone and metabolic research = Hormon- und Stoffwechselforschung = Hormones et metabolisme* **46**, 833-840, doi:10.1055/s-0034-1389955 (2014).
26 Calaghan, S., Kozera, L. & White, E. Compartmentalisation of cAMP-dependent signalling by caveolae in the adult cardiac myocyte. *J Mol Cell Cardiol* **45**, 88-92, doi:10.1016/j.yjmcc.2008.04.004 (2008).
27 Brannmark, C. *et al.* Adiponectin is secreted via caveolin 1-dependent mechanisms in white adipocytes. *J Endocrinol* **247**, 25-38, doi:10.1530/JOE-20-0078 (2020).
28 Musovic, S. & Olofsson, C. S. Adrenergic stimulation of adiponectin secretion in visceral mouse adipocytes is blunted in high-fat diet induced obesity. *Sci Rep* **9**, 10680, doi:10.1038/s41598-019-47113-8 (2019).
29 Gucek, A. *et al.* Fusion pore regulation by cAMP/Epac2 controls cargo release during insulin exocytosis. *eLife* **8:e41711**, doi:10.7554/eLife.41711 (2019).
30 Bates, R., Huang, W. & Cao, L. Adipose Tissue: An Emerging Target for Adeno-associated Viral Vectors. *Mol Ther Methods Clin Dev* **19**, 236-249, doi:10.1016/j.omtm.2020.09.009 (2020).
31 Moffat, J. & Sabatini, D. M. Building mammalian signalling pathways with RNAi screens. *Nature reviews. Molecular cell biology* **7**, 177-187, doi:10.1038/nrm1860 (2006).
32 Li, M. & Rossi, J. J. Lentiviral vector delivery of siRNA and shRNA encoding genes into cultured and primary hematopoietic cells. *Methods in molecular biology* **433**, 287-299, doi:10.1007/978-1-59745-237-3_18 (2008).
33 Carlotti, F. *et al.* Lentiviral vectors efficiently transduce quiescent mature 3T3-L1 adipocytes. *Mol Ther* **9**, 209-217, doi:10.1016/j.ymthe.2003.11.021 (2004).

Author contributions

MMS and CSO outlined the study and designed the experiments. MMS carried out all experimental work and analysis. CSO and MMS wrote the manuscript. SB provided method and analysis expertise and gave valuable input on the manuscript. All authors approved the final version of the manuscript.

Funding

This study was funded by the Swedish Research Council (2013-07107 and 2019-01239).

Legends

Fig.1 Model of cAMP and Ca^{2+} affects on adiponectin exocytosis in white adipocytes.
Forskolin and 3-isobutyl-1-methylxanthine (IBMX) elevate the intracellular concentration of cAMP through the activation of adenylyl cyclase (AC) and inhibition of phosphodiesterase, respectively. The elevation of cAMP results in activation of the downstream target Epac1 and fusion of adiponectin containing vesicles with the plasma membrane with subsequent adiponectin release. Ionomycin, a calcium ionophore, facilitates the transport of Ca^{2+} across the plasma membrane and the elevation in intracellular Ca^{2+} augments the release of pre-docked adiponectin containing vesicles at the plasma membrane. Ca^{2+} also induces replenishment of release-competent adiponectin vesicles, to maintain secretion of adiponectin over longer time periods.

Fig.2 Expression of adiponectin and shRNA-mediated adiponectin knockdown in 3T3-L1 adipocytes.
A) Gene expression of endogenous adiponectin in 3T3-L1 cells/adipocytes measured at every 48 hours after initiation of differentiation. Western blot **(B)** and densitometric analysis (**C**) of adiponectin protein expression after shRNA-mediated knockdown of endogenous adiponectin in 3T3-L1 cells. shRNAs significantly reduced adiponectin expression at protein level compared with control. The cells were infected with lenti-virus-expressing control shRNA targeting GFP (scrambled) and two variants of shRNA targeting murine adiponectin (shAcrp30-A and shAcrp30-C), and differentiated into mature adipocytes after puromycin selection. **D)** mRNA levels of adiponectin in shRNA-mediated knockdown compared with control cells. Statistical analysis: Brown-Forsythe and Welch ANOVA tests (Dunnett's T3 multiple comparisons test), assuming unequal SDs at α – level of 0.05 for A and Ordinary One-way ANOVA tests (Dunnett's multiple comparisons test), assuming equal SDs at α – level of 0.05 for C & D. Data are presented as mean ± SEM of three independent experiments. *P<0.05, ***P<0.001 and ****P<0.0001.

Fig.3 Rescue of shRNA-mediated adiponectin knockdown using lenti-viral infection with mCherry fused with human adiponectin in 3T3-L1 cells.
Western blot for **A)** reduced and **B)** non-reduced adiponectin. The expression of mCherry-fused adiponectin in the 3T3-L1 adipocytes was observed under **C)** Fluorescence (Scale bar= 100 µm) and **D)** TIRF microscope (Scale bar= 10 µm). The 3T3-L1 cells, with shRNA-mediated silencing of endogenous adiponectin expression, were infected with lenti-virus for stably expressing human adiponectin fused with mCherry at C-terminal alone or with FLAG-tag at either C- or N- terminal. The lenti-virus infected cells were differentiated and the over-expression of recombinant adiponectin was analysed.

Fig.4 TIRF imaging of cAMP-stimulated 3T3-L1 adipocyte adiponectin exocytosis.
3T3-L1 adipocytes stably expressing recombinant adiponectin were serum starved for 30 minutes at 32 ^{0}C and treated with **A**) 10 µM Forskolin and 200 µM IBMX and **B)** DMSO as Control for 15 minutes during which images were taken at 2 FPS using TIRF microscope. Laser wavelength of 561 nm with exposure time between 30 - 100 ms was used to excite mCherry. Note in inset region at lower panel that some vesicles are released (dotted circles) while others remain stable (whole circles). Scale bar=10 µm. **C)** Examples of Forskolin+IBMX-induced single vesicle dynamics over time, in the same cell and in the control. Scale bar= 2 µm. **D-E)** Relative average fluorescence intensity change vs. time in a single vesicle under Forskolin+IBMX stimulation. **F)** Cumulative frequency of percentage of vesicles released under Forskolin+IBMX stimulation showed nearly 60 % of vesicles released by the end of 10 minutes of co-stimulation. **G)** Vesicle count before and 15 minutes after stimulation with Forskolin+IBMX showed significant decrease in the number of vesicles after the co-stimulation. Statistical analysis: 2way ANOVA (Sidak's multiple comparisons test). Data are presented as mean ± SEM of eight independent experiments. *P<0.05; **P<0.01.

Fig.5 TIRF imaging of Ca^{2+}-stimulated 3T3-L1 adipocyte adiponectin exocytosis.
3T3-L1 adipocytes stably expressing recombinant adiponectin were serum starved for 30 minutes at 32 ^{0}C and treated with **A)** 1 µM ionomycin and **B)** DMSO as Control for 15 minutes during which images were taken at 2 FPS using TIRF microscope. Laser wavelength of 561 nm with exposure time between 30 - 100 ms was used to excite mCherry. Note in inset region at lower panel that some vesicles are released (dotted circles) while others remain stable (whole circles). Scale bar= 10 µm. **C)** Examples of ionomycin-induced single vesicle dynamics over time, in the same cell and in the control. Scale bar= 2 µm. **D-E)** Relative average fluorescence intensity change vs. time in a single vesicle under ionomycin stimulation. **F)** Cumulative frequency of percentage of vesicles released under ionomycin stimulation showed nearly 15 % of vesicles released by the end of 10 minutes of stimulation. **G)** Vesicles count before and 15 minutes after stimulation with ionomycin showed significant decrease in the number of vesicles after the stimulation. Statistical analysis: 2way ANOVA (Sidak's multiple comparisons test). Data are presented as mean ± SEM of eight independent experiments. *P<0.05; **P<0.01.

Fig.6 cAMP- and Ca^{2+}-stimulated adiponectin secretion in native and adiponectin-mCherry expressing 3T3-L1 adipocytes.
A) Native mature 3T3-L1 adipocytes were serum starved for 30 minutes at 32 ^{0}C and treated with DMSO, an adenylate cyclase activator (Forskolin) and phosphodiesterase inhibitor (IBMX), or Ca^{2+} ionophore (Ionomycin) for 30 minutes at 32 ^{0}C. The extracellular solutions were collected and analysed for endogenous total Adiponectin release using ELISA. Both co-stimulation with Forskolin and IBMX, and stimulation with Ionomycin significantly increased the secretion of total adiponectin compared to the control. Statistical analysis: Brown-Forsythe and Welch ANOVA (Dunnett's T3 multiple comparisons test), assuming unequal SDs at α – level of 0.05. N=6 for Control and Ionomycin; N= 5 for Forskolin+IBMX. **B)** Representative bright field image of mature 3T3-L1 adipocyte stably expressing recombinant adiponectin. Scale bar=10 µm. 3T3-L1 adipocytes stably expressing recombinant adiponectin were serum starved for 30 minutes at 32 ^{0}C and treated with DMSO, Forskolin and IBMX, and Ionomycin for 30 minutes at 32 ^{0}C. The extracellular solutions were collected and analysed for **C)** human total adiponectin and **D)** human HMW adiponectin using ELISA. Both co-stimulation with

Forskolin and IBMX, and stimulation with Ionomycin significantly increased the secretion of both human total and HMW adiponectin compared to the controls. Statistical analysis: Ordinary One-way ANOVA (Holm-Sidak's multiple comparisons test), assuming equal SDs at α – level of 0.05. N= 4. Data are presented as mean ± SEM. *P<0.05, **P<0.01 and ***P<0.001.

Table 1

Primer	Forward	Reverse
shAcrp30-A	CCGGCTACAACCAACAGAATCATTACTCGAGTAATGATTCTGTTGGTTGTAGTTTTTG	AATTCAAAAACTACAACCAACAGAATCATTACTCGAGTAATGATTCTGTTGGTTGTAG
shAcrp30-B	CCGGGACAAGGCCGTTCTCTTCACCCTCGAGGGTGAAGAGAACGGCCTTGTCTTTTTG	AATTCAAAAAGACAAGGCCGTTCTCTTCACCCTCGAGGGTGAAGAGAACGGCCTTGTC
shAcrp30-C	CCGGCCACAATGGCACACCAGGCCGCTCGAGCGGCCTGGTGTGCCATTGTGGTTTTTG	AATTCAAAAACCACAATGGCACACCAGGCCGCTCGAGCGGCCTGGTGTGCCATTGTGG
Acrp30	CCCAAGGGAACTTGTGCAGGTTGGATG	GTTGGTATCATGGTAGAGAAGAAAGCC
β-Actin	TTCTTTGCAGCTCCTTCG	TTCTGACCCATTCCCACC

Supplementary Videos

Supplementary video 1

3T3-L1 adipocytes stably expressing adiponectin-mCherry were treated with 10 µM Forskolin and 200 µM IBMX for 15 minutes during which images were taken at 2 FPS using TIRF microscope. The video is condensed to show every 10th frame. Time point of FSK/IBMX addition = 30 s. Scale bar = 10 µm.

Supplementary video 2

3T3-L1 adipocytes stably expressing recombinant adiponectin were treated with DMSO as control for 15 minutes during which images were taken at 2 FPS using TIRF microscope. The video is condensed to show every 10th frame. Scale bar = 10 µm.

Supplementary video 3

3T3-L1 adipocytes stably expressing recombinant adiponectin were treated with 1 µM ionomycin for 15 minutes during which images were taken at 2 FPS using TIRF microscope. The video is condensed to show every 10th frame. Time point of ionomycin addition = 30 s. Scale bar = 10 µm.

Supplementary video 4

3T3-L1 adipocytes stably expressing recombinant adiponectin were treated with DMSO as control for 15 minutes during which images were taken at 2 FPS using TIRF microscope. The video is condensed to show every 10th frame. Scale bar = 10 µm.

Abbreviation

AAV = Adeno-Associated Virus

ANOVA = Analysis of variance

ATCC = American Type Culture Collection

cAMP = Cyclic Adenosine Monophosphate

CMV = Cytomegalovirus

DMEM = Dulbecco's Modified Eagle Medium

DMSO = Dimethyl sulfoxide

EDTA = Ethylenediaminetetraacetic acid

EGFP = Enhanced Green Fluorescent Protein

ELISA = Enzyme-linked immunosorbent assay

Epac1 = Exchange factor directly activated by cAMP 1

Epac2 = Exchange factor directly activated by cAMP 2

EC = Extracellular

FBS = Fetal bovine serum

FPS = Frames per second

FSK = Forskolin

GFP = Green Fluorescent Protein

HMW = High Molecular Weight

IBMX = 3-isobutyl-1-methylxanthine

NPY = Neuropeptide Y

NS = Not significant

PAGE = Polyacrylamide gel electrophoresis

PVDF = Polyvinylidene fluoride

qPCR = quantitative polymerase chain reaction

ROI = Region of interest

SD = Standard deviation

SDS = Sodium dodecyl-sulfate

SEM = Standard error of mean

shRNA = short hairpin ribonucleic acid

TIRF = Total internal reflection fluorescence

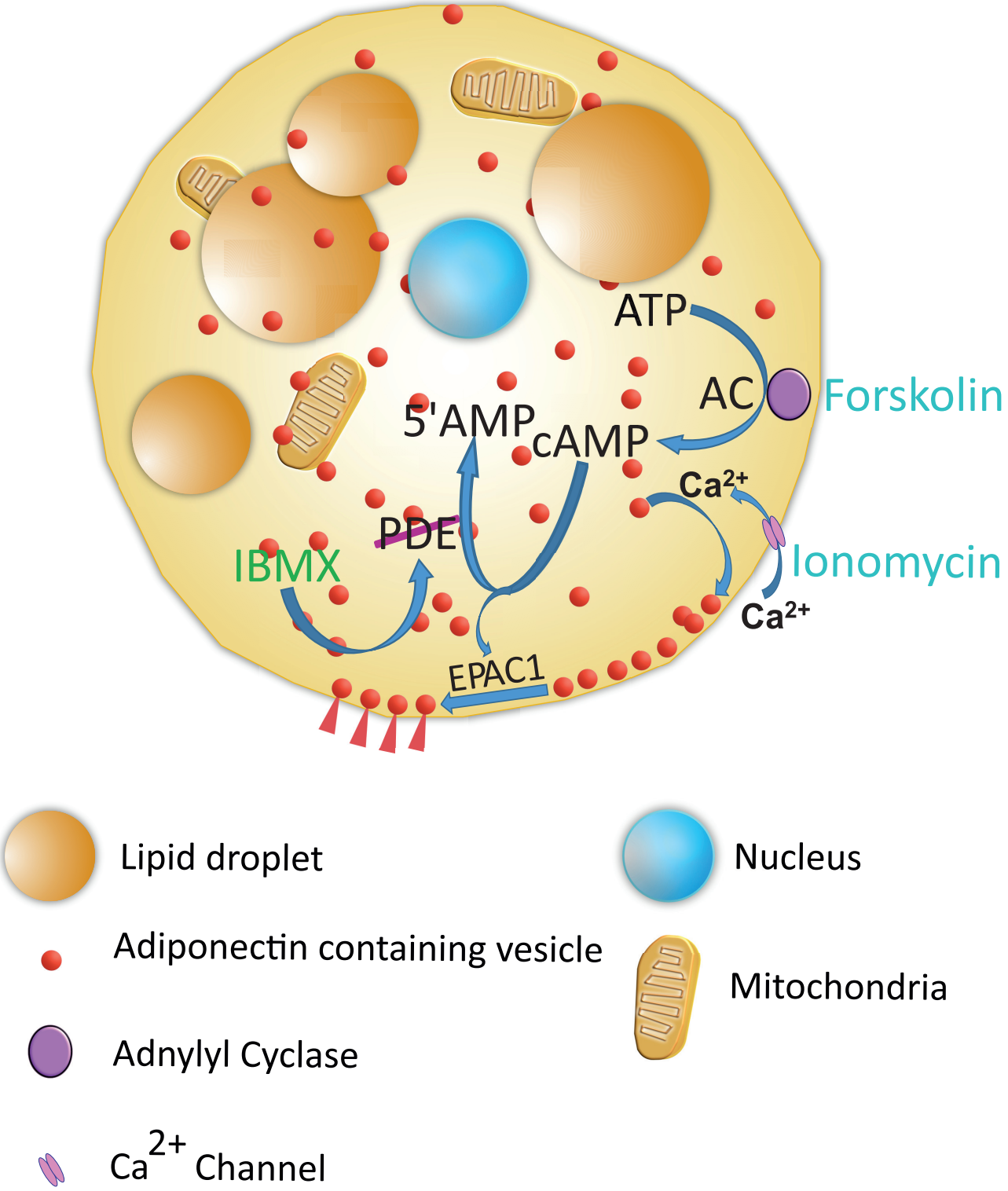
ATP
AC
Forskolin
5'AMP
cAMP
Ca2+
PDE
IBMX
Ionomycin
Ca2+
EPAC1
Lipid droplet
Nucleus
Adiponectin containing vesicle
Mitochondria
Adnylyl Cyclase
Ca2+ Channel

Fig. 1

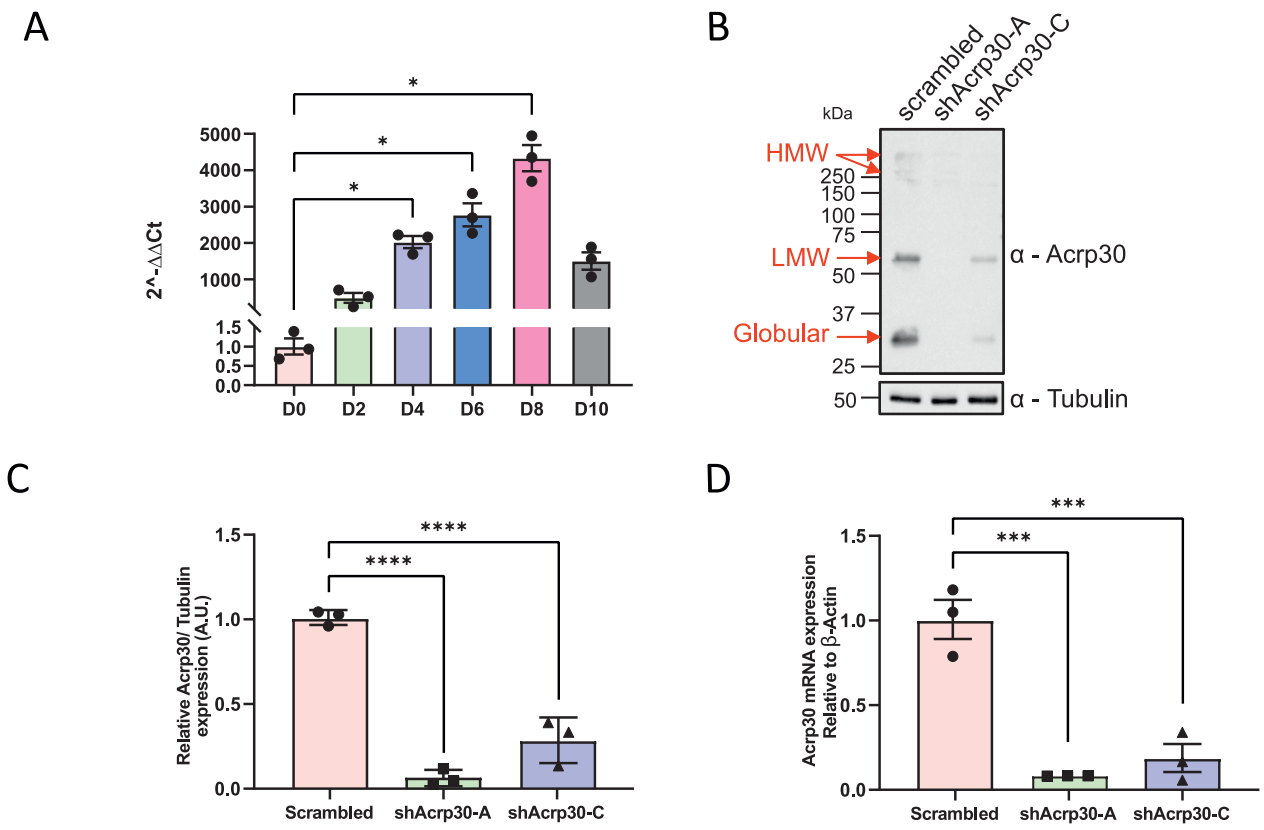
A
2^-ΔΔCt
5000
4000
3000
2000
1000
1.5
1.0
0.5
0.0
D0
D2
D4
D6
D8
D10
B
scrambled
shAcrp30-A
shAcrp30-C
kDa
HMW
250
150
100
75
LMW
50
37
Globular
25
50
α - Acrp30
α - Tubulin
C
Relative Acrp30/ Tubulin expression (A.U.)
Scrambled
shAcrp30-A
shAcrp30-C
D
Acrp30 mRNA expression Relative to β-Actin
Scrambled
shAcrp30-A
shAcrp30-C

Fig. 2

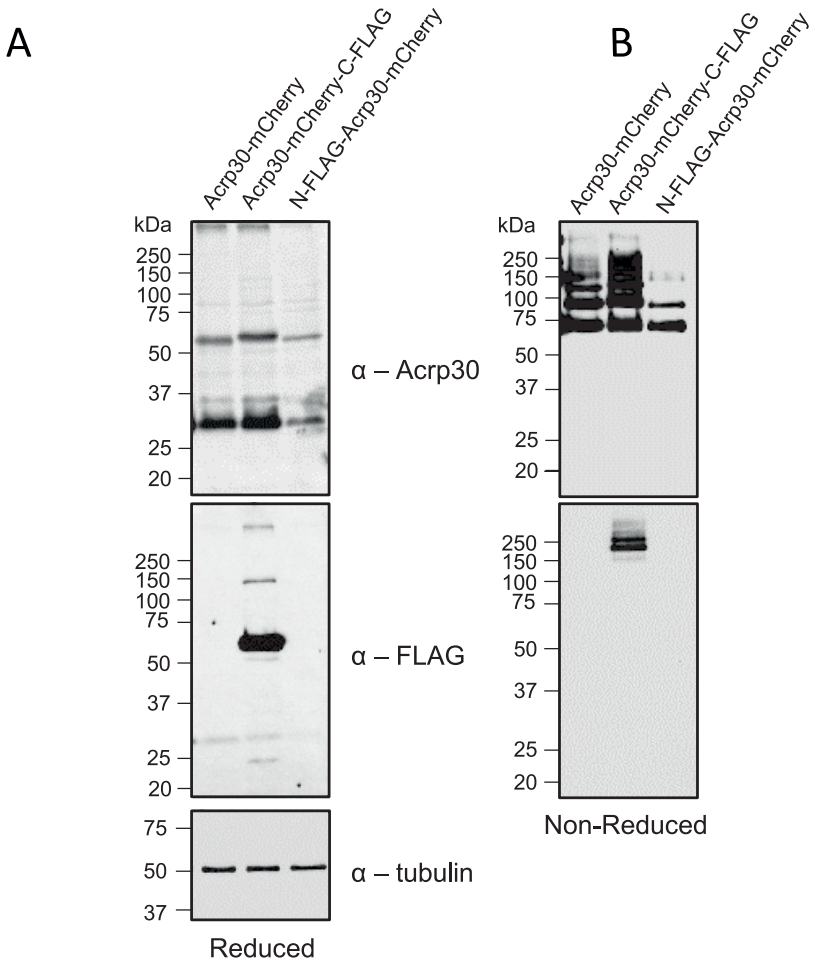
A
B
Acrp30-mCherry
Acrp30-mCherry-C-FLAG
N-FLAG-Acrp30-mCherry
kDa
250
150
100
75
50
37
25
20
α – Acrp30
α – FLAG
α – tubulin
Reduced
Non-Reduced

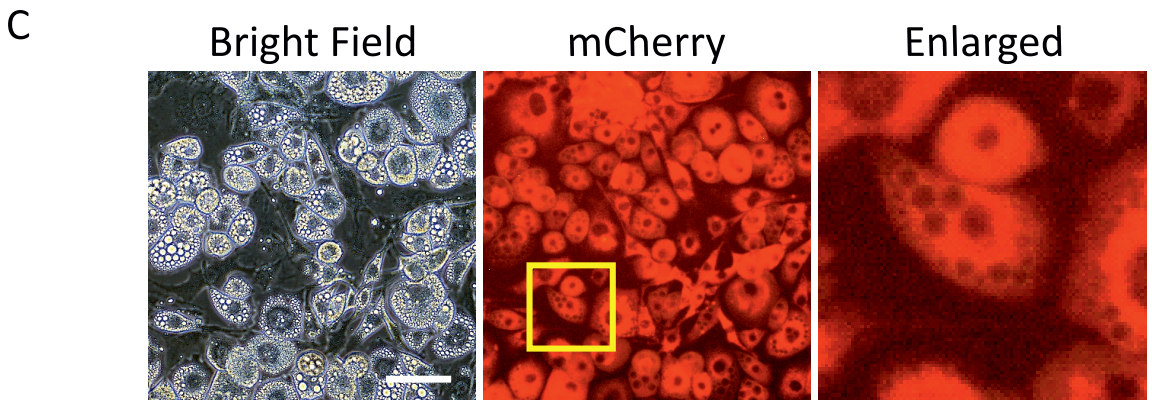
C
Bright Field
mCherry
Enlarged

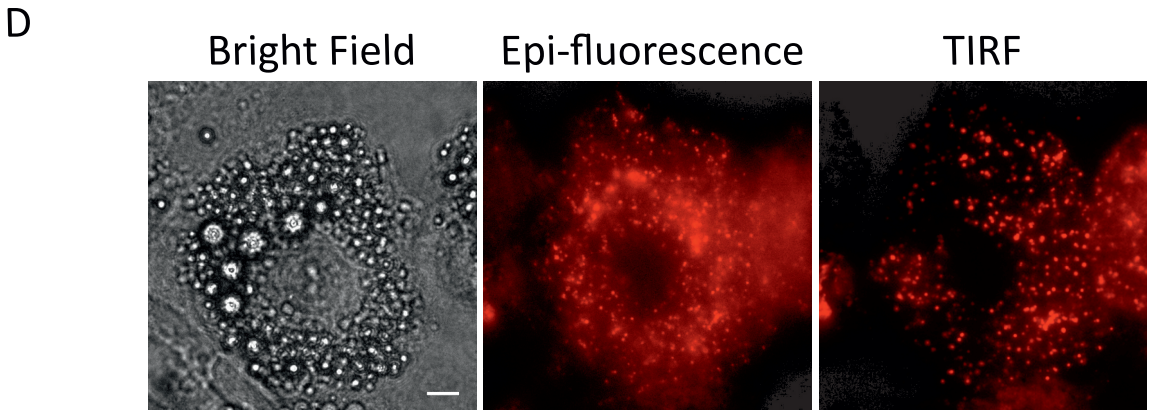
D
Bright Field
Epi-fluorescence
TIRF

Fig. 3

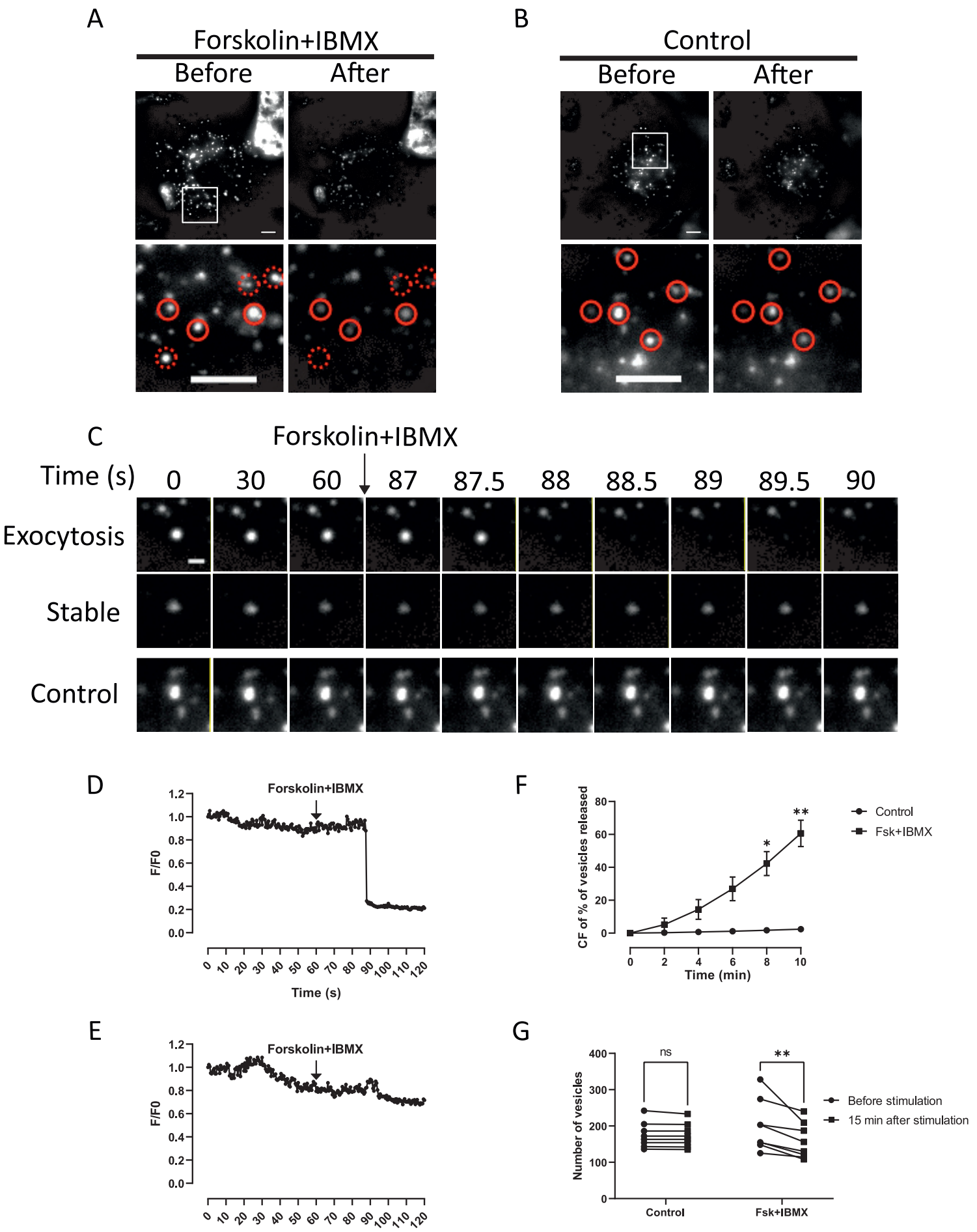
A
Forskolin+IBMX
Before
After
B
Control
Before
After
C
Forskolin+IBMX
Time (s)
0
30
60
87
87.5
88
88.5
89
89.5
90
Exocytosis
Stable
Control
D
Forskolin+IBMX
F/F0
Time (s)
E
Forskolin+IBMX
F/F0
F
CF of % of vesicles released
Time (min)
Control
Fsk+IBMX
G
Number of vesicles
ns
**
Control
Fsk+IBMX
Before stimulation
15 min after stimulation

Fig. 4

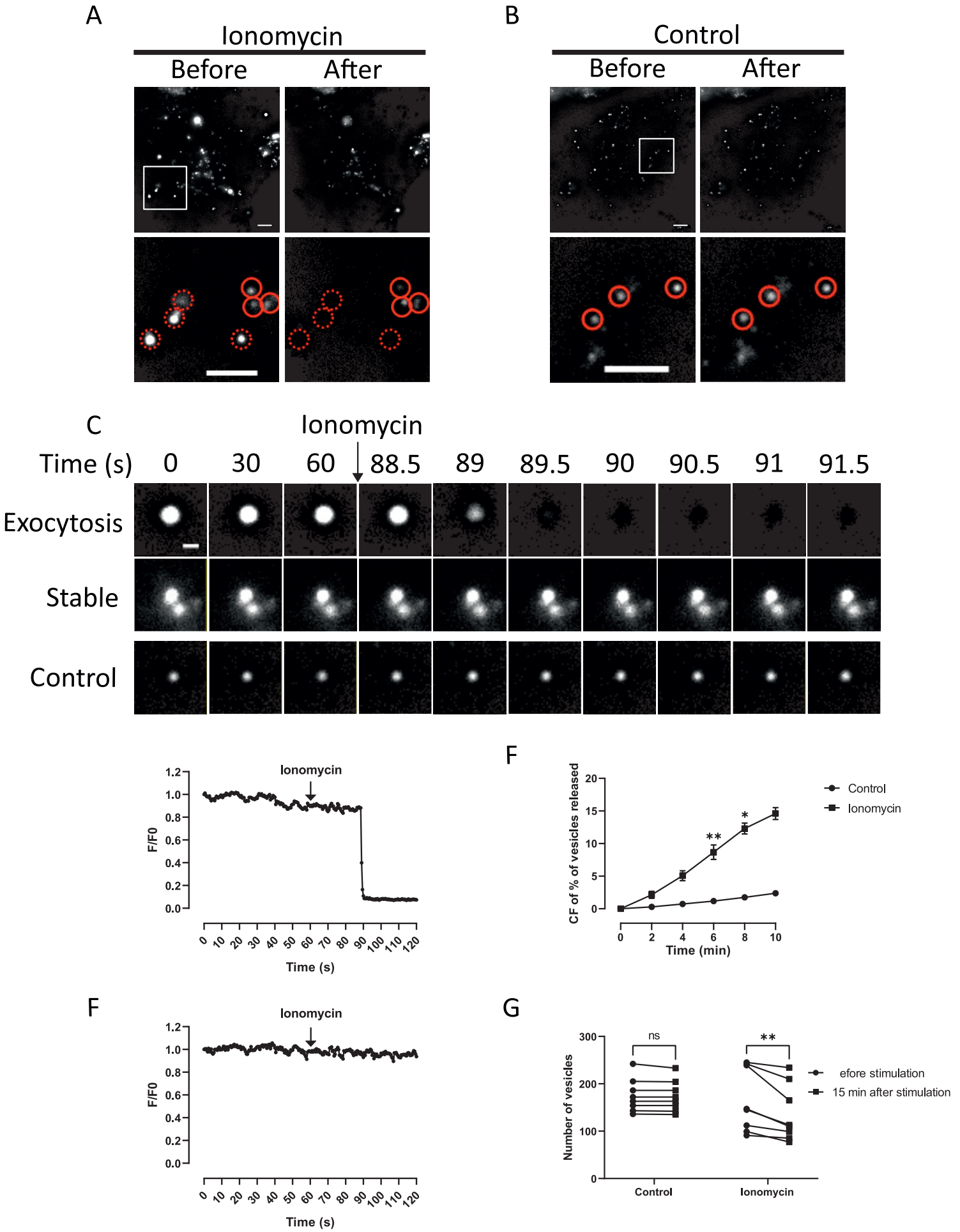
A
Ionomycin
Before
After
B
Control
Before
After
C
Ionomycin
Time (s)
0
30
60
88.5
89
89.5
90
90.5
91
91.5
Exocytosis
Stable
Control
Ionomycin
F/F0
Time (s)
F
CF of % of vesicles released
Time (min)
Control
Ionomycin
F
Ionomycin
F/F0
Time (s)
G
Number of vesicles
ns
**
efore stimulation
15 min after stimulation
Control
Ionomycin

Fig. 5

A

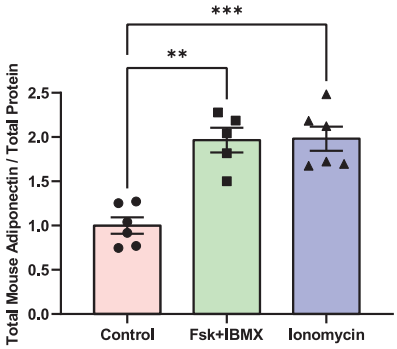
***
**
Total Mouse Adiponectin / Total Protein
2.5
2.0
1.5
1.0
0.5
0.0
Control
Fsk+IBMX
Ionomycin

B

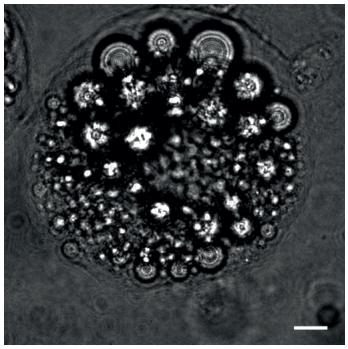

C

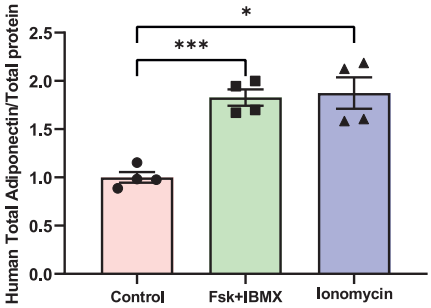
*
***
Human Total Adiponectin/Total protein
2.5
2.0
1.5
1.0
0.5
0.0
Control
Fsk+IBMX
Ionomycin

D

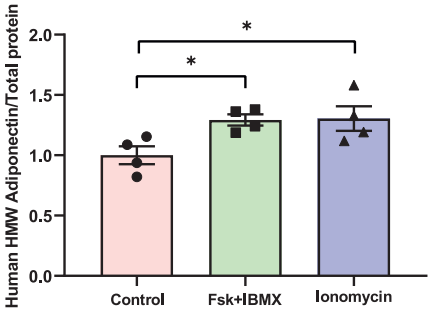
*
*
Human HMW Adiponectin/Total protein
2.0
1.5
1.0
0.5
0.0
Control
Fsk+IBMX
Ionomycin

Fig. 6

Supplementary Fig 1

A

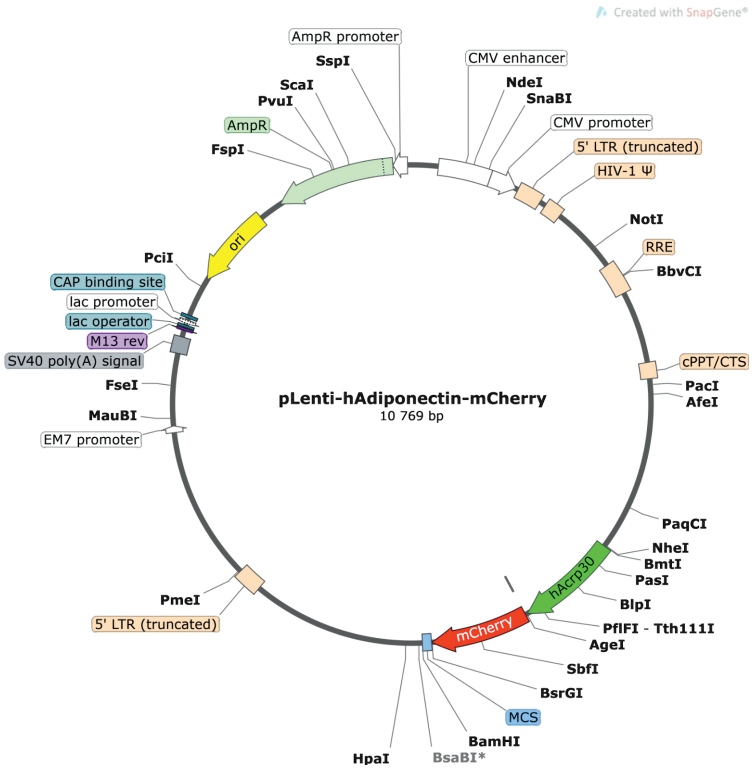

B

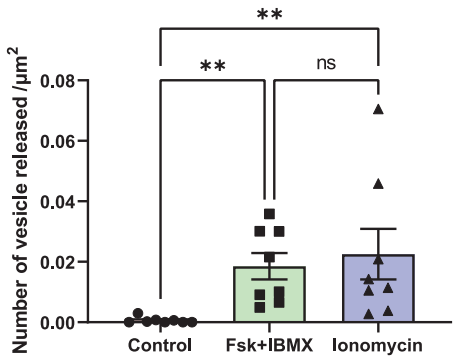

A) Plasmid map of lenti-viral construct for human adiponectin fused with mCherry at C-terminal created with SnapGene. 3T3-L1 adipocytes expressing recombinant adiponectin were serum starved for 30 minutes at 32 ^{0}C and treated with 10 µM Forskolin and 200 µM IBMX, 1 µM ionomycin and DMSO as Control for 15 minutes at 32 ^{0}C during which images were taken at 2 FPS using TIRF microscope. **B)** Number of vesicles released per square µm cell area under the stimulations significantly increased with both co-stimulation with Forskolin and IBMX, and stimulation with Ionomycin compared to the controls. The effect of cAMP- and Ca^{2+}-elevating agents was analysed using the Kruskal-Wallis test with Dunn's multiple comparisons test. Data are presented as mean ± SEM of eight independent experiments. ** P<0.01, ns= not significant.